scientific reports

Check for updates

OPEN

Network pharmacology and metabolomics reveal mathurameha, a Thai traditional Anti-Diabetic formula, enhances glucose metabolism through PI3K-AKT/AMPK/GLUT4 pathway modulation

Subhadip Banerjee[1], Wuttichai Jaidee[1], Narawadee Rujanapun[1], Thidarat Duangyod[1,2], Tharakorn Maneerat[1,4], Pravaree Phuneerub[1,2], Kulwadee Malee[1], Siam Popluechai[4,15], Virayu Suthiphasilp[5], Panupong Puttarak[6,7], Poonsit Hiransai[8,9], Surat Laphookhieo[3,4], Salfarina Ramli[10,11], Wim Vanden Berghe[12], Geoffrey A. Cordell[13,14] & Rawiwan Charoensup[1,2,16]✉

Traditional herbal formulations offer promising avenues for diabetes management by targeting multiple molecular pathways. Mathurameha (MT), a polyherbal preparation, has been historically used for its antidiabetic potential. However, its molecular mechanisms remain largely unexplored. FrE exhibited potent α-glucosidase inhibition (IC_{50} 0.3 µg/mL) and significantly enhanced glucose uptake in L6 myotubes (3.67 ± 0.23-fold) and 3T3-L1 adipocytes (IC_{50} 6.78 µg/mL). It also stimulated insulin secretion (1.42-fold), comparable to metformin (1.46-fold), and protected INS-1 pancreatic β-cells from H_2O_2-induced apoptosis (30.65 ± 3.54%) through partial caspase-3 inhibition. LC-MS-QTOF analysis identified 73 metabolites, including ellagic acid, kushenol A, gallic acid, arctiin, neoandrographolide, astilbin, paenol, muricatacin, coumarrayin, and zingerone. Network pharmacology and pathway enrichment analyses revealed key targets (GSK3β, GLUT4, PPARG, INSR, AKT2, CASP3, and MMP9) and highlighted the involvement of PI3K-AKT, AMPK, and GLUT4 signaling pathways. Gene expression analysis confirmed the upregulation of GLUT4, AMPK, IRS, PI3K, and AKT genes in L6 myotubes treated with FrE. These findings suggest that MT exerts antidiabetic effects via the PI3K-AKT/AMPK/GLUT4 signaling axis, promoting glucose uptake, insulin secretion, and β-cell protection. Future studies will focus on in vivo validation, standardization of bioactive fractions, and omics-based approaches to establish a well-defined, effective formulation for diabetes management.

Keywords Mathurameha, Thai traditional medicine, Twenty-six medicinal plant mixture, Antidiabetic activity, Glucose transport, LC-MS/MS-QTOF analysis, Network pharmacology, Insulin secretion enrichment

Abbreviations

MT	Mathurameha
PI3K	phosphoinositide-3-kinase
AKT	*β* serine/threonine-protein kinase
AMPK	activated protein kinase
AMY2	Alpha-amylase
AMY2A	pancreatic alpha-amylase
CA2	Carbonic Anhydrase II
CASP3	Caspase-3
DAPk1	death-associated protein kinase

GLUT4	Glucose transporter type 4
GSK3β	glycogen synthase kinase
GLP1R	glucagon-like peptide-1 receptor
DPP4	dipeptidyl peptidase 4
IGF1R	insulin-like growth factors
INSR	insulin receptor
2 NBDG	2-(N-(7-Nitrobenz-2-oxa-1,3-diazol-4-yl)-amino)−2-deoxyglucose
MMP9	Matrix metallopeptidase 9
PRKCA	protein kinase C alpha
PPARG	peroxisome proliferator gamma
SGLT2	sodium/glucose cotransporter 2
T2DM	type 2 Diabetes Mellitus
IRS	Insulin receptor substrate

[1]Medicinal Plant Innovation Center of Mae Fah Luang University, Mae Fah Luang University, Chiang Rai 57100, Thailand. [2]School of Integrative Medicine, Mae Fah Luang University, Chiang Rai 57100, Thailand. [3]Center of Chemical Innovation for Sustainability (CIS) and School of Science, Mae Fah Luang University, Chiang Rai 57100, Thailand. [4]School of Science, Mae Fah Luang University, Chiang Rai 57100, Thailand. [5]Department of Industrial Technology and Innovation Management, Faculty of Science and Technology, Pathumwan Institute of Technology, Bangkok 10330, Thailand. [6]Phytomedicine and Pharmaceutical Biotechnology Excellence Center, Faculty of Pharmaceutical Sciences, Prince of Songkla University, Hat-Yai 90110, Songkhla, Thailand. [7]Department of Pharmacognosy and Pharmaceutical Botany, Faculty of Pharmaceutical Sciences, Prince of Songkla University, Hat-Yai 90110, Songkhla, Thailand. [8]Center of Excellence in Marijuana, Hemp, and Kratom, Walailak University, Nakhon Si Thammarat 80160, Thailand. [9]School of Allied Health Sciences, Walailak University, Nakhon Si Thammarat 80160, Thailand. [10]Faculty of Pharmacy, Universiti Teknologi MARA Cawangan Selangor, Puncak Alam 42300, Selangor, Malaysia. [11]Integrative Pharmacogenomics Institute (iPROMISE), Universiti Teknologi MARA Cawangan Selangor, Puncak Alam 42300, Selangor, Malaysia. [12]Laboratory for Protein Chemistry, Proteomics & Epigenetic Signalling (PPES), Department of Biomedical Sciences, University of Antwerp, Wilrijk 2610, Belgium. [13]Natural Products Inc., Evanston, IL 60201, USA. [14]College of Pharmacy, University of Florida, Gainesville, FL 32610, USA. [15]Gut Microbiome Research Group, Mae Fah Luang University, Muang, Chiang Rai 57100, Thailand. [16]Medicinal Plant Innovation Center of Mae Fah Luang University and School of Integrative Medicine, Mae Fah Luang University, Chiang Rai 57100, Thailand. ✉email: rawiwan.cha@mfu.ac.th

Type 2 Diabetes Mellitus (T2DM) is a chronic condition characterized by high blood glucose levels due to the impaired regulation of glucose by insulin[1]. The global prevalence of T2DM has risen dramatically in recent decades, driven by genetic predisposition and lifestyle factors, such as high-fat/high-glucose diets, sedentary behaviour, and chronic stress[2]. These factors contribute to persistent glucose spikes, leading to prolonged insulin secretion, pancreatic β-cell dysfunction, and insulin resistance, ultimately exacerbating disease progression[3]. Despite the availability of pharmacological interventions - including metformin, sulfonylureas, and GLP-1 receptor agonists - many patients experience side effects, limited efficacy in advanced stages, or treatment non-adherence due to cost, accessibility, and cultural preferences[4]. Consequently, there is growing interest in complementary and alternative medicines (CAM), particularly polymedicinal plant formulations, which are used traditionally in diverse medical systems worldwide[5].

Medicinal plants have long been investigated for their antidiabetic properties, with recent studies highlighting their ability to regulate key metabolic pathways, enhance insulin sensitivity, and provide pancreatic β-cell protection[6–8]. For instance, Marsupsin, isolated from the polyplant product ABPA, was shown to rejuvenate insulin resistance in skeletal muscle cells by activating the IRS1-PI3K-AKT-GLUT4 pathway, underscoring its potential to improve glucose metabolism[8]. Similarly, several Thai medicinal plants demonstrated α-glucosidase inhibitory activity, supporting their role in glycemic control[7]. The traditional Thai formulation Mathurameha (MT) has exhibited promising glucose-lowering effects in preclinical models[9–11]. However, their translational potential for wider applications remains limited by insufficient mechanistic insights, a gap addressed by recent advances in systems and integrative pharmacology. For example, studies on complex medicinal plant anti-obesity formulations[12,13] and the Tibetan complex Compound Ruteng[14] employed molecular and computational approaches to dissect the operating mechanisms, offering frameworks for characterizing traditional medicinal plant-based therapies. Similarly, the cardioprotective effects of the Chinese Erzhi Pill against diabetic complications were examined through integrative methods[15]. These efforts highlight the critical need for comprehensive molecular characterization to bridge traditional knowledge with mechanistic assessments, ensuring the clinical relevance of medicinal plant-based interventions.

One such promising complex medicinal plant-based formulation is Mathurameha (MT), a Thai traditional medicine composed of 26 medicinal plants (**Table S1**). MT is currently prescribed in Thailand (300 mg, twice daily) for T2DM management, particularly for newly diagnosed patients with fasting blood sugar (FBS) levels below 220 mg/dL, obesity (BMI > 30), and individuals younger than 60 years old[9,16]. Preliminary studies indicated that an aqueous extract of MT exerts significant glucose-lowering effects in streptozotocin-nicotinamide (STZ-Na)-induced diabetic rats, outperforming ethanolic extracts in oral glucose tolerance tests (OGTT), and showed no acute toxicity on male and female rats at a dose as high as 5 g/kg b.w[9]. Previous studies in this laboratory demonstrated that MT mitigates high-glucose-induced endothelial dysfunction through the EGF/NO/IL-1β regulatory axis[16]. Furthermore, an ethanol extract of MT modulated adipose tissue morphology and prevented fat accumulation in vascular tissues, indicating a broader spectrum of bioactive metabolites than aqueous extract[17]. Therefore, it became important to elucidate the role of the MT ethanol extract components for their

actions on the diverse aspects of the pathological progression of diabetes. This research approach is crucial to meet the need for a deeper understanding of how complex medicinal plant formulations interact and regulate cellular pathways and biological targets.

In this study, MT was systematically characterized applying a multi-modal molecular approach. Ethanol and aqueous extracts were prepared, followed by bioactivity-guided fractionation of the ethanol extract into polarity-based fractions, and LC-MS/MS QTOF metabolomic analysis was performed. These extracts and fractions were evaluated for α-glucosidase and α-amylase inhibition, glucose uptake enhancement in L6 myotubes and 3T3-L1 adipocytes, and their ability to stimulate insulin secretion and protect pancreatic β-cells from oxidative stress. Finally, network pharmacology analysis of the most bioactive fraction (FrE) was integrated with gene expression profiling to elucidate the key molecular targets. This study builds on a previous proteomic and in vivo investigation[16,18], and aims to provide deeper mechanistic insights into the antidiabetic potential of MT, contributing to the science-based development of this traditional formulation.

Methods

Materials and instruments

Methanol, ethyl acetate, hexane, ethanol, and dichloromethane (AR grade, Thermo Fisher Scientific, Waltham, MA, USA) were used for extraction and fractionation. Water, formic acid, and acetonitrile (LC-MS grade, Sigma-Aldrich, Burlington, MA, USA) were used for the LC-MS-QTOF analysis. The mobile phase was filtered using membrane filters (Millipore, 0.45 μm pore size, Merck KGaA, Darmstadt, Germany), and MT extracts were filtered using syringe filters (0.45 μm Millipak Express filter and 0.22 µm membrane filter for particulate-free and bacteria-free water, Merck KGaA, Darmstadt, Germany), and a Büchi rotary vacuum evaporator (R-200, CH-9230 Flawil, Switzerland) were used.

Acquisition of the Mathurameha formulation

The medicinal plants listed in **Table S1** were purchased from Ayurawet Wattana Medicine Limited Partnership, Phichit, Thailand, and stored at room temperature (ca. 27–30 °C). Quality control assessment was carried out using physico-chemical methods. Microscopic examination, loss on drying, moisture content, extractive values, water content, volatile oil content, total ash, acid-insoluble ash, heavy metal content and total plate count were assessed by Ayurawet Wattana Medicine Limited Partnership, Phichit, Thailand following the Thai Herbal Pharmacopoeia 2021 and supplement 2022 protocols. Specimens of the 26 medicinal plants (voucher nos. MPIC/MT/22/05–31) were deposited in the Medicinal Plant Innovation Centre, Mae Fah Luang University, Chiang Rai, Thailand. The plant materials were each thoroughly washed with water; shade dried, and ground to a powder using an electronic mixer grinder (Mitsubishi CM, Charatchai Machinery Ltd., Bangkok, Thailand). The powdered crude drugs were combined according to the established formula to obtain the MT formulation.

Extraction and fractionation

Powdered MT mixture (1.0 kg) was successively extracted for 24 h at room temperature with EtOH (3 × 1 L) and distilled water (3 × 1 L). Following filtration, the EtOH extracts were combined and evaporated under reduced pressure to afford the crude EtOH extract (104.4 g, 26%). The combined aqueous extracts were freeze-dried, yielding the aqueous extract (18.5 g, 9.3%). The extracts were stored at 4 °C until tested in the biological assays and the LC/QTOF-MS analysis. Given the promising results in the safety and glucose uptake assays (Figs. 1a-b), the crude EtOH extract was further fractionated. The crude EtOH extract (104.4 g) was dissolved in water (500 mL) and partitioned with hexane (500 mL, 3 times) to remove chlorophyll and the lipophilic constituents. The hexane extract was evaporated under reduced pressure to yield a hexane-soluble fraction (FrH) (1.99 g). The aqueous portion was further partitioned successively with dichloromethane, EtOAc, and *n*-butanol (each 500 mL). The extracts were evaporated under reduced pressure to yield a dichloromethane fraction (FrD) (1.54 g), an EtOAc fraction (FrE) (40.6 g), and a *n*-butanol fraction (FrB) (1.42 g) (see Supplementary Material, Scheme 1).

α-Glucosidase and α-Amylase Inhibition activity

The α-glucosidase and α-amylase inhibitory effects of the MT samples were assessed as described[19]. MT sample concentrations were 25, 50, 100, 250, and 500 µg/mL of the EtOH extract, water extract, FrD, FrE, and FrB. Acarbose (3.125–250 µg/mL) was utilized as the positive control for both assays as it inhibits both enzymes and is prescribed to manage postprandial hyperglycemia[20].The absorbance reactions were measured using a microplate reader (EnVision, Perkin Elmer, Waltham, MA, USA). The IC_{50} values were determined by plotting the inhibition percentages of the samples at various concentrations in an Excel spreadsheet and fitting a trendline to the data. The concentration at which the trendline indicates 50% inhibition corresponds to the IC_{50} value.

Cell culture and treatment conditions

Three cell models were utilized: 3T3-L1 pre-adipocytes (ATCC® CL-173™): Cultured in DMEM (3 mg/mL glucose) supplemented with 10% FBS, 2 mM glutamine, and 1% penicillin/streptomycin at 37 °C under 5% CO_2. L6 myotubes (ATCC® CRL-1458™): Maintained in DMEM (10% FBS, 1% penicillin/streptomycin) at 37 °C in 95% air/5% CO_2. Differentiation into multinucleated myotubes was induced by switching to DMEM with 2% FBS at 80% confluence, with media changes every 48 h over 7 days. INS-1 pancreatic β-cells: Cultured as previously described[19]. Cells were treated with MT ethanol/water extracts or the polarity-based fractions (FrB, FrD, and FrE; 25–100 µg/mL) for 24 h. Metformin (CAS: 1115-70-4) (1-755 µM) served as a positive control.

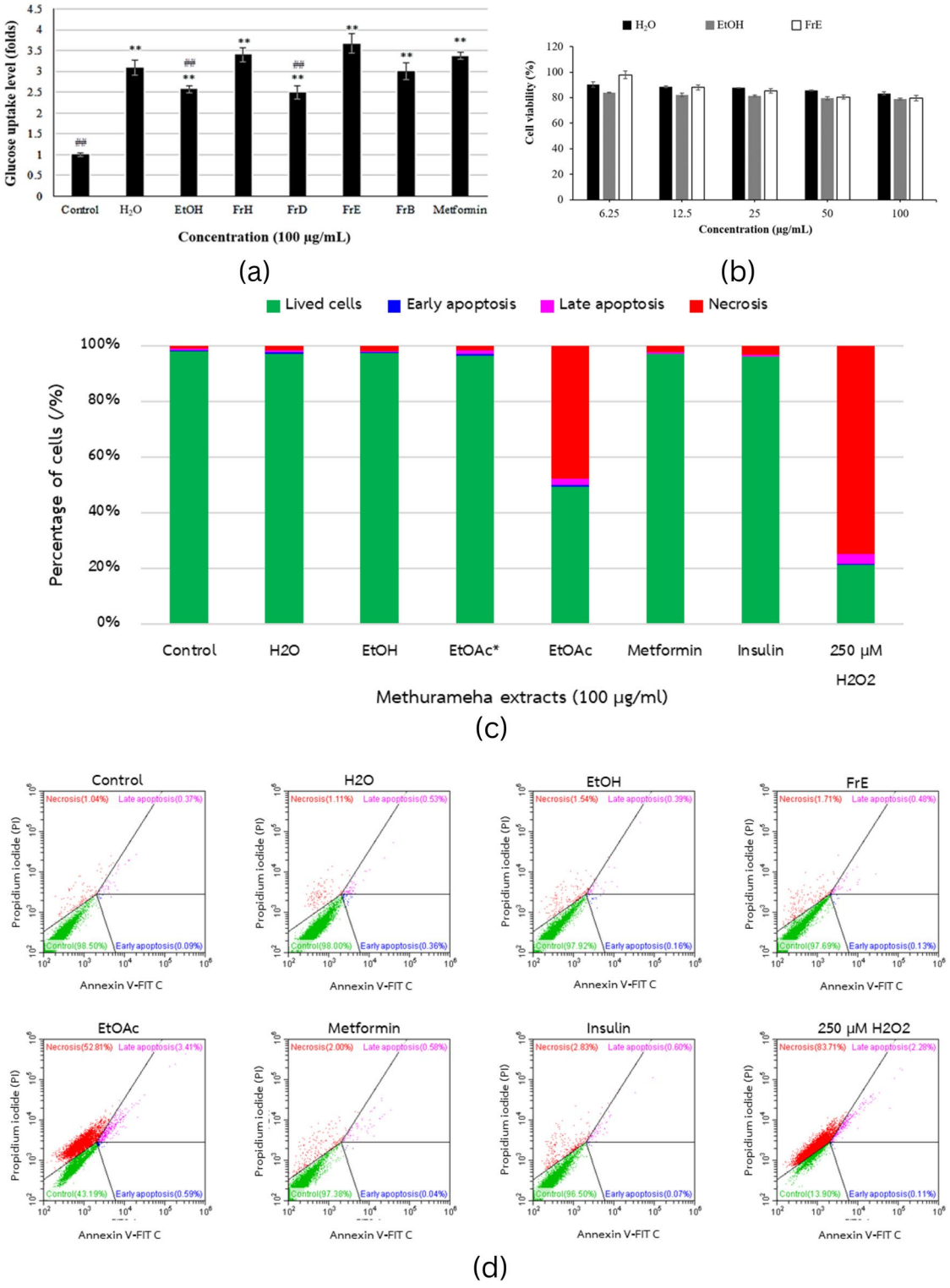

Fig. 1. Experimental Assessment of antidiabetic potential of MT. **(a)** The effect of MT remedy extracts and fractions on the stimulation of glucose uptake on L6 myotube cells. One-way ANOVA followed by Tukey test; ** $P<0.001$ compared with control, ## $P<0.001$ compared with metformin. **(b)** INS-1 pancreatic β-cell viability after treatment with MT remedy extracts and FrE. Apoptosis assay using flow cytometry after staining with annexin V-FITC/propidium iodide (PI). INS-1 cells were treated with 250 μM H_2O_2 for 48 h to induce hypoxic stress mediated apoptosis. The effect of MT extracts and FrE in apoptosis protection on INS-1 cells. **(c)** Percentage of viable, early apoptotic and late apoptotic cells. (d) Representative scatter plots of PI (y-axis) vs. annexin V(x-axis).

Cell viability assay
Cells (4×10^4/well in 96-well plates) were treated with MT samples for 24 h, followed by incubation with 0.5 mM MTT for 4 h. Formazan crystals were solubilized in DMSO (100 µL/well), and the absorbance was measured at 570 nm using a microplate reader (EnVision, Perkin Elmer). Viability was normalized to untreated controls[20].

Glucose uptake in L6 myotubes
Differentiated myotubes were exposed to MT samples for 24 h, washed with Kreb's Ringer buffer solution, and incubated with 80 µM 2-NBDG fluorescent glucose analog for 60 min. Fluorescence intensity (485/530 nm excitation/emission) was quantified to assess the glucose uptake.

Glucose consumption in 3T3-L1 adipocytes
Adipocytes were treated with the MT samples in glucose-enriched medium (3 mg/mL) for 24 h. Residual glucose was quantified using a glucose oxidase/peroxidase assay (510 nm absorbance). IC_{50} values were derived from the dose-response curves.

Insulin secretion in INS-1 β-Cells
Cells were stimulated with 1000 mg/mL glucose post-MT treatment. Supernatants were analyzed using the AlphaLISA Insulin Detection Kit (Perkin Elmer), with luminescence measured at 615 nm.

Caspase-3 activity assay
H_2O_2-Stressed INS-1 cells (250 µM, 24 h) were lysed, and caspase-3 activity was quantified using Ac-DEVD-pNA substrate (CASP3C Kit, Sigma-Aldrich). Absorbance at 405 nm was proportional to enzymatic activity[21].

Apoptosis detection through flow cytometry
H_2O_2-treated INS-1 cells were stained with Annexin V-FITC/PI (ANNEXIN V: FITC Kit, Bio-Rad) and analyzed on a DxFlex flow cytometer (Beckman Coulter). Apoptotic (Annexin V^+/PI^-) and necrotic (Annexin V^+/PI^+) populations were quantified using CyExpert 2.5 software[22].

Statistical analysis
Data were analyzed in GraphPad Prism 8.0.1. All experiments were performed in triplicate. Statistical analysis was conducted using one-way ANOVA followed by Tukey's post hoc test, with p-values < 0.05 considered significant.

LC/QTOF-MS analysis
The phytochemical constituents of the MT extracts were investigated using a LC-MS-QTOF-ESI-MS instrument (Agilent 6500 Series, Santa Clara, CA, USA). A small amount of the mobile phase ACN-H_2O (1:1%v/v) was used to dissolve and dilute all samples to a concentration of 200 µg/mL.Before chromatographic analysis, the material was re-filtered through a 0.22 m PTFE membrane syringe filter. The chromatographic separation was conducted using an Agilent Zorbax Eclipse Plus - C18 column (2.1 × 50 mm, 1.8 μm) eluting with water containing 0.1% formic acid (A) and acetonitrile (0.1% formic acid) (B) as the mobile phase. The flow rate was 1 mL/min: 5% mobile phase B for one minute, increasing linearly to 17% B in 13 min. The eluent was increased to 100% mobile phase B within 22 min, and the eluent composition was then held steady for two minutes before being reduced to 5% mobile phase B over two minutes. Both positive and negative ion modes were used in the mass range m/z 100–1000 amu. Identification of the chromatographic peaks was performed by matching retention times and mass spectra to compounds in the library using the PCDL database (TCM-database, phenolic acids, and Pubchem chemical database) with a high accuracy (error < 5 ppm). MS/MS fragment matching was performed for each identified component[23]. Mass Profiler Professional (Agilent, Santa Clara, CA, USA) was used to perform chemometric differential MS-data analysis to derive the relationship between the extracts and their bioactivity. The retention times (RT), predicted and measured errors (in ppm), m/z values, chemical formulae, sigma values (an exact numerical comparison between the theoretical and measured isotope patterns), and MS/MS fragmentation patterns were used to identify the chemical components. Molecular feature extraction was applied to determine the metabolites in the EtOH extract (Pos 1389, Neg-656), the H_2O extract (Pos-558, Neg-1527), and FrE (Pos-248, Neg-150). Compounds were identified using the height of 100,000, RT > 3.3, and a mass error of < 5 ppm to confirm their elemental composition.

Network Pharmacology analysis
Metabolites identified as present in the FrE fraction were subjected to target prediction using BindingDB (threshold 0.7)[24]SwissTargetPrediction (> 0.1)[25], and LigTMap[26]. Human target IDs with UniProtKB references were retrieved. SwissADME[27] analysis assessed oral bioavailability and druggability (Table S4). Venny 2.1 was used for Venn diagram analysis. The corresponding targets identified were searched in DisGeNet[28] to identify 701 unique diabetes-associated genes. Protein-protein interaction (PPI) analysis was performed using STRING, and hub-module topology was examined through NetworkAnalyst (http://www.networkanalyst.ca)[29,30]. Functional annotation of molecular targets was assessed through DAVID 6.8[31], incorporating pathways from Gene Ontology, KEGG[32,33]and BioCarta[34]. Network enrichment was analyzed using MCODE[35,36]with scoring based on physical interactions from Biogrid[37,38]. Cytoscape was employed for network visualization, mapping hierarchical target relationships and protein-protein interaction linkages[39,40].

Sample	α-Glucosidase inhibition	α-Amylase inhibition
	IC_{50} (μg/mL)	
EtOH extract	5.41 ± 0.1	17.45 ± 0.5
Aqueous extract	13.5 ± 0.1	210.8 ± 2.3
Fraction FrH	11.0 ± 0.1	> 250.0
Fraction FrD	14.5 ± 0.8	21.0 ± 2.2
Fraction FrE	0.3 ± 0.0	23.5 ± 1.3
Fraction FrB	1.6 ± 0.4	47.2 ± 2.2
Acarbose	146.0 ± 1.2	57.7 ± 1.5

Table 1. α-Glucosidase and α-amylase inhibitory activities of MT samples.

MT Sample	3T3-L1 Cell viability (%) at 100 μg/mL MT samples	Concentration that inhibits 50% of glucose consumption IC_{50} (μg/mL)
EtOH extract	82.09 ± 1.16^{a}	28.97^{a}
Aqueous extract	$83.80 \pm 0.55^{a, b}$	12.02^{b}
Fraction FrH	$83.91 \pm 0.65^{a, b}$	$> 100^{c}$
Fraction FrD	$82.92 \pm 0.65^{a, b}$	$> 100^{c}$
Fraction FrE	$83.65 \pm 0.80^{a, b}$	6.78^{d}
Fraction FrB	$81.40 \pm 1.37^{a, b}$	$> 100^{c}$
Metformin	84.14 ± 1.15^{b}	21.19^{a}

Table 2. Effect of MT extracts and fractions on cell viability and glucose uptake in 3T3-L1 cells. One-way ANOVA followed by Tukey test; $p < 0.05$ compared with Metformin the values with different superscript letters in a column are significantly different ($p < 0.05$).

Quantitative PCR for gene expression analysis

Based on the network analysis results, PCR analysis was carried out to investigate the expression of genes in glucose metabolism. L6 cells were treated with MT extracts and metformin (100 μg/mL). mRNA (1 μg) was transformed to cDNA using a cDNA synthesis kit. PCR was performed using specific primers (Fig. 7). The amplified cDNA products were separated electrophoretically using a 1% agarose gel. Normalization with the GAPDH gene as the internal control was used to calculate the relative expression level of a target gene. The ImageJ program (National Institutes of Health, Bethesda, MD, USA) was used to quantify the gene expression.

Results

In vitro antidiabetic activity of MT extracts and fractions

Glucose control in diabetes involves inhibiting α-glucosidase and α-amylase to reduce postprandial glucose, enhancing muscle glucose consumption, increasing insulin secretion, and protecting pancreatic β-cells from oxidative damage. The EtOH and aqueous extracts, along with fractions obtained from the EtOH extract, the hexane (FrH), dichloromethane (FrD), ethyl acetate (FrE), and *n*-butanol (FrB) fractions, were evaluated for their antidiabetic effects using the abovementioned assays.

Enzyme Inhibition assay

The results presented in Table 1 showed that the FrE and EtOH extracts exhibited the lowest IC_{50} values for inhibiting α-glucosidase and α-amylase, respectively. All of the MT samples and acarbose inhibited α-glucosidase more effectively than α-amylase, except for the aqueous extract and FrH, which showed weak or no inhibition of α-amylase. These observations indicate that the constituents in these extracts do not interact with α-amylase. The superior inhibition of α-glucosidase aligns with previous reports that α-amylase inhibition is limited by poor ligand binding affinities to high molecular weight ligands compared to α-glucosidase[41].

Glucose consumption and uptake assay

In the glucose consumption and uptake assays (Tables 2 and 3), high viability of 3T3-L1 (81.4–83.9%) and L6 myotubes (86.2–97.7%) was observed when exposed to MT samples for 24 h, indicating the absence of acute cytotoxic effects. Among all the MT samples, FrE exhibited the most potent effects on glucose uptake and consumption. In the glucose consumption assay, measured using the GOD-POD assay, FrE inhibited 50% of glucose consumption by 3T3-L1 adipocytes at a concentration of 6.78 μg/mL, followed by the aqueous extract. The inhibition effects of both were better than metformin (Table 2). In the glucose uptake assay, all MT samples increased glucose uptake in L6 myotubes compared to control (Table 3). FrE significantly enhanced glucose uptake beyond metformin (Fig. 1a), whereas the aqueous and EtOH extracts showed lower activity than metformin.

Samples (100 µg/mL)	Cell viability L6 at 100 µg/mL (%)	Glucose uptake(Folds)
Control	86.77 ± 5.51[a]	1.0 ± 0.05[a]
Aqueous Extract	90.34 ± 4.12[a, b]	2.48 ± 0.03[b]
EtOH Extract	89.64 ± 3.45[a, b]	2.56 ± 0.10[b]
FrH	86.59 ± 1.12[a]	3.40 ± 0.17[c]
FrD	91.12 ± 0.40[a, b]	2.49 ± 0.16[b]
FrE	97.74 ± 2.39[b]	3.67 ± 0.23[c]
FrB	86.20 ± 3.54[a]	2.49 ± 0.16[b]
Metformin	84.51 ± 1.51[a]	3.37 ± 0.07[c]

Table 3. Effect of MT extracts and fractions on cell viability and glucose consumption of L6 myotubes. One-way ANOVA followed by Tukey test; $p < 0.05$ compared with Metformin the values with different superscript letters in a column are significantly different ($p < 0.05$).

Samples	Insulin secretion		
	Concentration		Fold induction
	(µg/mL)	(µIU/mL)	
EtOH extract	0.61 ± 0.008[a]	2063.96 ± 34[a]	1.21 ± 0.017[a]
Aqueous extract	0.55 ± 0.005[b]	1856.26 ± 20[b]	1.11 ± 0.010[b]
Fraction FrE	0.71 ± 0.005[c]	2512.11 ± 26[c]	1.42 ± 0.012[c]
Control	0.50 ± 0.009[d]	1641.90 ± 34[d]	1.00 ± 0.018[d]
Metformin	0.73 ± 0.011[e]	2611.33 ± 52[e]	1.46 ± 0.022[e]

Table 4. The effects of MT aqueous extract, the EtOH extract, and FrE on insulin secretion. One-way ANOVA followed by Tukey test; $p < 0.05$ compared with Metformin the values with different superscript letters in a column are significantly different ($p < 0.05$).

Sample	Caspase-3 activity	
	pNA (µM)	Caspase-3 inhibition (%)
EtOH extract	1262.00 ± 6.92[a]	8.77 ± 0.50[a]
Aqueous extract	1149.33 ± 17.92[b]	16.92 ± 1.30[b]
Fraction FrE	959.33 ± 49.00[c]	30.65 ± 3.54[c]
Caspase-3	2464.00 ± 31.24[d]	-
Untreated cells	430.00 ± 10.58[e]	-
H_2O_2-Treated cells	1383.33 ± 63.00[f]	-
Metformin	483.33 ± 32.15[e]	65.06 ± 2.32[d]

Table 5. The effects of MT aqueous extract, EtOH extract and FrE on caspase-3 activity. The values with different superscript letters in a column are significantly different ($p < 0.05$).

Insulin secretion and β-Cell protection

Based on the promising effects observed in Tables 1, 2 and 3, the insulin secretion activities of the aqueous extract, the EtOH extract, and the FrE fraction were examined. Table 4 shows that the MT samples increased insulin secretion compared to the control, metformin. FrE enhanced insulin secretion to 2512.11 ± 26 µIU/mL, comparable to metformin ($p > 0.05$). To assess pancreatic β-cell protection, hypoxic stress was induced in INS-1 β-cells using 250 µM of H_2O_2, followed by treatment with the aqueous extract, the EtOH extract, and FrE for 24 h. Flow cytometry results showed that FrE significantly reduced H_2O_2-induced apoptosis (Figs. 1b-d). Furthermore, caspase-3 activation, a key indicator of apoptosis, was quantified by measuring *p*-nitroaniline (pNA) release after hydrolysis of the Ac-DEVD-pNA substrate (Table 5). FrE significantly reduced caspase-3 activity (30.65 ± 3.54%), though its protective effect was less than that of metformin (65.06 ± 2.32%). FrE exhibited superior anti-apoptotic effects compared to the EtOH and aqueous extracts, as shown by partial caspase-3 inhibition in INS-1 β-cells under H_2O_2-induced hypoxic stress (Table 5). These results suggest that MT extracts, especially FrE, protect against caspase-3-mediated apoptosis in pancreatic β-cells.

Phytochemical characterization of the MT aqueous extract, the EtOH extract, and FrE by LC-MS-QTOF chemometrics

Based on the biological assays results, the LC-MS/MS analyses of the H_2O and EtOH extracts, and FrE were carried out. Table 6 summarizes the LC-MS/MS parameters of the metabolites from FrE, while the compounds present

Sl. No.	Compound Name	Diff (DB, ppm)	Molecular Formula	Mass	m/z	RT (min)	Phytochemical Class
1	Gallic acid	−1.78	$C_7H_6O_5$	170.0218	169.0146	2.59	Phenolic acid
2	Strictinin	−0.08	$C_{27}H_{22}O_{18}$	634.0807	633.0734	10.09	Ellagitannin
3	Amlaic acid	0.19	$C_{27}H_{24}O_{19}$	652.0911	651.0838	10.37	Polyphenol
4	4-Hydroxycoumarin	1.08	$C_9H_6O_3$	162.0315	163.0387	11.84	Coumarin derivative
5	Ellagic acid	0.17	$C_{14}H_6O_8$	302.0062	300.9989	13.78	Polyphenol
6	Tomentosin	−0.4	$C_{34}H_{24}O_{22}$	784.0762	785.0835	14.13	Tannin
7	Isoterchebin	−0.93	$C_{41}H_{30}O_{27}$	954.0983	476.0419	14.17	Tannin
8	(+)−3,3',5',5,7-Pentahydroxyflavanone	−1.75	$C_{15}H_{12}O_7$	304.0588	305.0661	15.62	Flavonoid
9	γ-Heptalactone	0.31	$C_7H_{12}O_2$	128.0837	187.0975	15.85	Lactone
10	Tellimagrandin I	−0.66	$C_{34}H_{26}O_{22}$	786.0921	787.0995	15.88	Tannin
11	(+)−3,3',5',5,7-Pentahydroxyflavanone	−0.92	$C_{21}H_{22}O_{11}$	450.1166	449.1094	16.10	Flavonoid
12	Cryptomerin B	3.9	$C_{32}H_{22}O_{10}$	566.1191	625.1329	16.80	Lignan
13	Bellamarine	−2.42	$C_{18}H_{19}NO_4$	313.1322	314.1395	16.92	Alkaloid derivative
14	Clerodin	0.46	$C_{20}H_{30}O_5$	350.2092	385.1786	17.01	Terpenoid
15	Muricatacin	−0.37	$C_{17}H_{32}O_3$	284.2352	329.2335	17.49	Fatty acid derivative
16	Tecostanine	−0.75	$C_{11}H_{21}NO$	183.1625	242.1764	17.51	Alkaloid
17	Arctiin	−0.19	$C_{27}H_{34}O_{11}$	534.2102	579.2085	17.54	Lignan glycoside
18	Rutamarin	−3.17	$C_{21}H_{24}O_5$	356.1635	357.1708	17.54	Coumarin derivative
19	Neoandrographolide	0.21	$C_{26}H_{40}O_8$	480.2722	525.2704	17.61	Diterpenoid glycoside
20	Glyuranolide	4.76	$C_{31}H_{44}O_6$	512.3114	571.3252	17.82	Sesquiterpene lactone
21	Schisanlactone E	−0.53	$C_{30}H_{44}O_4$	468.3242	469.3314	17.82	Triterpenoid
22	Eleutherin	−1.49	$C_{16}H_{16}O_4$	272.1053	273.1127	18.74	Quinonoid compound
23	Ethyl cinnamate	−0.07	$C_{11}H_{12}O_2$	176.0837	194.1176	19.36	Phenylpropanoid ester
24	α-Obscurine	−1.36	$C_{17}H_{26}N_2O$	274.2049	309.1743	19.54	Alkaloid
25	Cinnamic acid	−4.25	$C_9H_8O_2$	148.0531	149.0603	19.62	Phenylpropanoid acid
26	Artemisic acid	1.04	$C_{15}H_{22}O_2$	234.1617	233.1545	20.17	Sesquiterpenoid
27	Argentatin F	−0.16	$C_{30}H_{42}O_3$	450.3135	485.2825	20.34	Triterpenoid
28	Kushenol A	0.1	$C_{25}H_{28}O_5$	408.1936	407.1864	20.45	Flavonoid
29	Cucurbitacin E	−1.09	$C_{32}H_{44}O_8$	556.3042	579.2934	20.57	Triterpenoid
30	Coumurrayin	−1.19	$C_{16}H_{18}O_4$	274.1208	275.1281	20.60	Coumarin derivative
31	Citronellyl acetate	−2.96	$C_{12}H_{22}O_2$	198.1626	199.1699	20.76	Monoterpenoid ester
32	Caudatin	3.52	$C_{27}H_{40}O_7$	476.2757	477.2831	20.89	Steroidal glycoside
33	16-Acetylgitoxigenin	3.77	$C_{25}H_{36}O_6$	432.2496	433.2568	20.95	Cardenolide
34	Mammeisin	0.11	$C_{25}H_{26}O_5$	406.178	405.1706	21.15	Xanthone

Table 6. The 34 metabolites identified from the LC-MS/MS-QTOF analysis of the Ethyl acetate fraction (FrE) of the ethanolic extract of Mathurameha (MT).

in the EtOH and H_2O extracts are summarized in Tables S2-S3, Figure S2-S5. The Total Ion Chromatograms (TIC) of the MS spectra of FrE are presented in Fig. 2a. where the metabolites were identified (numbered as Table 6) using the height of 100,000, RT > 3.3, and a mass error of < 5 ppm to confirm their elemental composition. The metabolites which represented artefact-matching scores from non-natural sources and synthetic fragments were identified manually from PubChem, Scifinder, and ChemSpider, and were not considered for further network pharmacology analysis.

Chemometric analysis of the MS data was performed for the MS-based differential analysis to determine the relationships of metabolites in the EtOH and H_2O extracts and FrE with the bioactivities evaluated in this study. The bioactivities are glucose consumption, insulin secretion, and caspase-3 inhibition. The Venn diagram (Fig. 2b) analysis showed that 12 compounds were common to all of the extracts, whereas 10 compounds in the FrE and 19 compounds in the H_2O extract were extractive specific. Hierarchical clustering (Fig. 2c) of the compounds from the different extracts was done based on their normalized intensity values with sample variability- CV < 25.0. Clustering was conducted on different experiments measuring the similarity based on Euclidean distancing following the Wards linkage rule for class prediction. The clustering results showed that kushenol A, gallic acid, ellagic acid, coumurrayin, and neoandrographolide contributed to the bioactivity of FrE and the aqueous extract.

Network Pharmacology identifies the MT constituents targeting diabetes-related proteins

Network pharmacology analysis revealed significant binding similarities between the FrE constituents and the diabetes-associated targets (**Fig. S1**). A Venn diagram (Fig. 3a) highlighted the FrE targets overlapping across the BindingDB, SwissTargetPrediction, and LigTmap databases. The target-compound network (1844 edges, 745

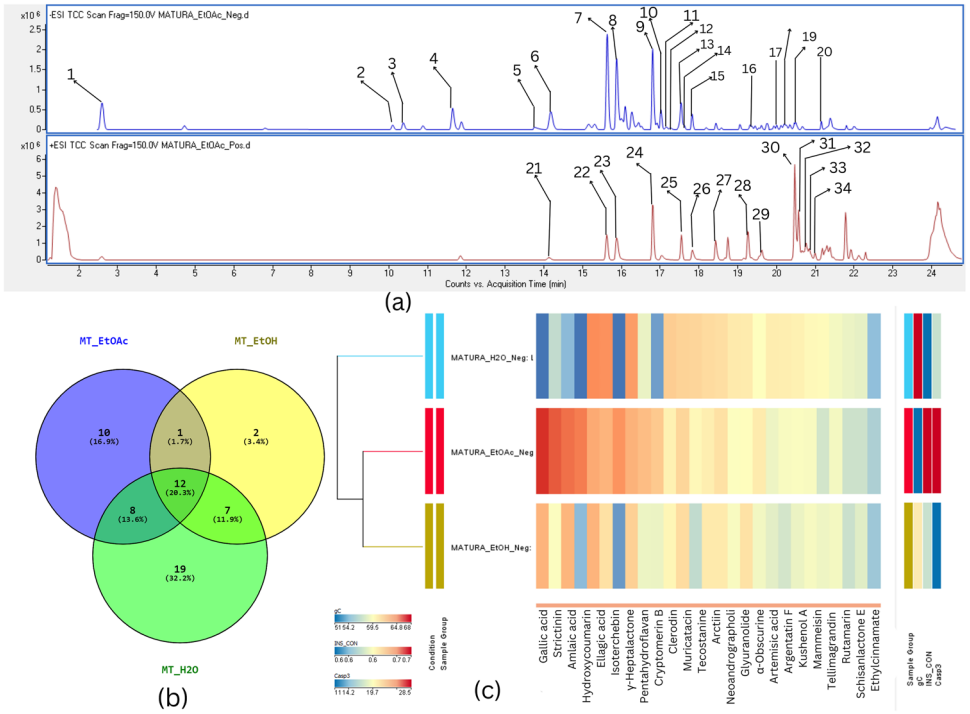

Fig. 2. Metabolite profiling of MT. **(a)** Total Ion Chromatogram (TIC) of different extracts and FrE (EtOAc fraction of EtOH). **(b)** Venn diagram analysis of compounds identified by LC-MS/MS different extracts and fractions. **(c)** Hierarchical clustering of the metabolites from different extracts based on different bioactivities.

nodes) identified hub proteins including MAPK14 (degree = 20), CA2 (20), PPARG (15), GSK3B (11), AMY2A (10), and CASP3 (6). Kinases, hydrolases, and G-protein-coupled receptors emerged as prominent targets, with key interactions observed for kushenol A, clerodin, and neoandrographolide. Notably, cinnamic acid, gallic acid, and strictinin targeted AMY2A, aligning with FrE's α-amylase inhibitory activity[41]. SwissADME-based ADME profiling (Fig. 3b, **Table S4**) indicated favorable drug-likeness for most metabolites (average bioavailability score = 0.6; Lipinski violations = 0.16). Compounds such as gentianose and arctiin exhibited lower bioavailability and higher violations (Ghose = 1.54, Muegge = 1.02), suggesting reduced druggability. FrE constituents, including ethyl cinnamate and gallic acid, interacted with carbonic anhydrase isoforms (CA1, CA2, CA4, etc.), implicated in hepatic gluconeogenesis[42,43]. Tankyrase1 (TNKS1), a regulator of GLUT4-mediated insulin sensitivity, was also targeted, suggesting modulation of adipocyte glucose uptake[44]. The PPI-enriched pathways are shown in Table 7. The low p values in Table 7 (< 0.05) indicating the enrichment of the KEGG pathway[32,33] or protein-protein interaction (PPI) network is unlikely to have occurred by chance, while a low FDR value (< 0.05) indicated that the results are reliable and that the false discovery rate is low. Pathways showing highly significant results include the MAPK signalling pathway (p-value = 1.29E-28), the FoxO signalling pathway (p-value = 8.09E-19), the HIF-1 signalling pathway (p-value = 9.65E-19), the PI3K-Akt signalling pathway (p-value = 1.09E-18), and the insulin signalling pathway (p-value = 2.87E-16).

STRING-based PPI analysis (Fig. 4a) revealed enrichment in insulin signalling (GO:0032869), glucose transport, and catalytic activity. MCODE clustering identified critical hubs (PIK3CA, INSR, IGF1R) linked to the NRF2-ARE and PI3K/AKT pathways (Figs. 4c-d). Figures 4b-d show the enriched network clusters based on enrichment scores of pathway terms and genetic ontology terms which were used in the network of pathways and process enrichment analyses. The enriched terms were clustered according to their kappa scores with a similarity > 0.3, and nodes reflecting significant p-values from each of the top clusters are connected by edges. The top clusters of the enriched terms are shown in Table 8, where "Count" is the number of query genes associated with each ontology term. The number for "%" represents the percentage of all query genes that are present in the specified ontology term. The multi-test adjusted p-value in log base 10 is known as "Log10(q)" and is computed using the previously mentioned procedures. The term "GO:0043408 responses to peptide" refers to any process that causes a change in the state or activity of a cell, including movement, secretion, enzyme production, and gene expression, in response to a peptide stimulus that may be insulin-mediated. GO:1,901,652 denotes the regulation of MAPK, which is important for promoting the transcription of the genes encoding the glucose transporters, GLUT1 and GLUT4[45]. P38/MAPK also boosts insulin-dependent glucose transport and increases glucose transfer that is insulin-independent[45]. PGC1 is induced by p-38/MAPK, which also increases oxidative metabolism, by co-activating mitochondrial biogenesis and activity. Interestingly, the "energy sensors" of the cell, AMPK and p38/MAPK, are co-expressed in the contracting skeletal muscle. The combined actions of these two kinases boost glucose import through a different insulin-dependent mechanism[46]. Experimental validation confirmed FrE-induced upregulation of IRS and AKT in L6 myotubes (Figs. 5a-b) and INS-1 cell

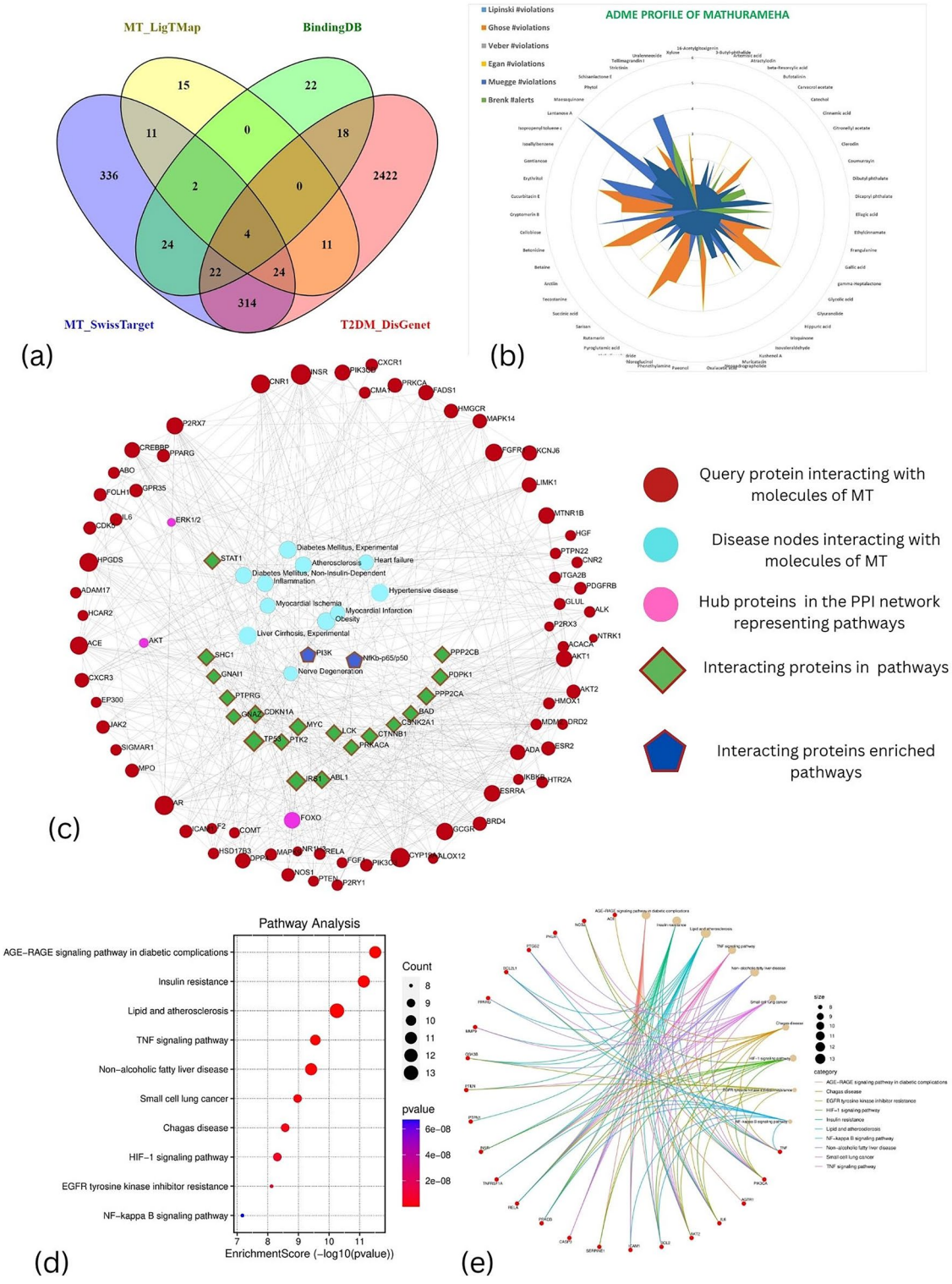

Fig. 3. Target Space Analysis and druggability of MT metabolites and targets. **(a)** Venn diagram of targets with diabetes-associated target space. **(b)** Radial graph of ADME profile. **(c)** Target-PPI–disease network showing the interaction between the Target proteins to diabetes and associated targets through protein-protein interaction analysis. **(d)** Pathway enrichment score plot. **(e)** Target-pathway network showing the targets in red circles and pathways in light orange sized based on enrichment. The edges represent separate pathways.

Pathway	*p*-Value	FDR
MAPK signalling pathway	1.29E-28	2.06E-26
FoxO signalling pathway	8.09E-19	2.86E-17
HIF-1 signalling pathway	9.65E-19	3.07E-17
PI3K-Akt signalling pathway	1.09E-18	3.15E-17
Pancreatic cancer	2.98E-18	7.29E-17
ErbB signalling pathway	3.69E-18	8.37E-17
Endocrine resistance	8.42E-18	1.67E-16
Insulin signalling pathway	2.87E-16	3.65E-15
Insulin resistance	1.18E-15	1.21E-14
TNF signalling pathway	1.81E-15	1.69E-14
AGE-RAGE signalling pathway in diabetic complications	2.46E-15	2.24E-14
AMPK signalling pathway	8.08E-10	4.67E-09
Wnt signalling pathway	3.92E-05	0.000121
RIG-I-like receptor signalling pathway	5.64E-05	0.000171
Adrenergic signalling in cardiomyocytes	6.58E-05	0.000197

Table 7. Enrichment of PPI KEGG pathways by MT (FrE). FDR- False discovery rate.

protection (Fig. 1b), supporting insulin signalling restoration through TCPTP inhibition. DAVID functional clustering (24 clusters, highest score = 7.2) highlighted PI3K-AKT, mTOR, and AMPK pathways (Figs. 6a-f) using KEGG databases[32]. Key targets (PIK3CA, AKT2, GSK3B) interacted with 16-acetylgitoxigenin, ellagic acid, and clerodin, modulating GLUT4-mediated glucose uptake. Crosstalk between AMPK and PI3K-AKT signalling was linked to reduced gluconeogenesis (through PTPN1) and improved insulin sensitivity[47,48].

PCR determination of the MT-dependent regulation of glucose metabolism gene expression

Based on the in silico prediction that the MT fractions regulate glucose metabolism through modulation of PI3K-AKT/AMPK/GLUT4 signalling, quantitative PCR gene expression analysis of GLUT4, AMPK, PI3K, AKT, and IRS in MT-treated L6 cells was performed to test this hypothesis. The results showed that L6 myotubes had high levels of GLUT4 and AMPK expression after treatment with the MT extracts, and FrE provided the most significant up-regulation. In addition, up-regulation was observed for IRS, PI3K, and Akt gene expression in cells treated with MT extracts (Figs. 6a,-**b**).

Discussion

The antidiabetic potential of the MT extracts, particularly the ethyl acetate fraction (FrE) of the ethanol extract, lies in its broad capacity to simultaneously target enzymatic, metabolic, and cellular pathways critical for diabetes pathogenesis. Building on recent advances in this laboratory[16,17] in elucidating the therapeutic mechanisms of traditional medicinal plant formulas, this study demonstrates that FrE outperforms conventional therapies, like metformin and acarbose, by integrating α-glucosidase inhibition, glucose transport modulation, β-cell protection, and insulin signalling enhancement and represents a multi-target strategy essential for addressing the multifactorial nature of diabetes. Previous studies, including Aluksanasuwan et al.. (2024)[16] and Somsuan et al.. (2024)[17]established a foundation for this investigation by employing SWATH-proteomics to decode the vascular protective effects of MT, through the EGF/NO/IL-1β axis. These studies revealed how medicinal plant mixtures can restore endothelial homeostasis in hyperglycemic environments, bridging in vitro pathway dissection[16] with the in vivo evaluation of cardiovascular protection in diabetic rats[17]. Here, this translational framework is applied to MT, leveraging its structural diversity and multi-target engagement to regulate glucose metabolism and mitigate diabetic complications. By combining high-resolution proteomics, network pharmacology, and functional assays, this work begins to address a critical gap in diabetes research, namely the need for therapeutic regimens that can holistically target both hyperglycemia and its systemic sequelae, while advancing the integration of traditional medicine into evidence-based, precision therapeutics.

Significance of enzyme Inhibition by MT in diabetes control

The in vitro findings establish that the MT extract exhibits holistic antidiabetic effects, surpassing metformin and acarbose by influencing multiple glucose regulation pathways. The α-glucosidase and α-amylase inhibition profiles of the MT extracts highlight their role in postprandial glucose control. Since α-glucosidase, primarily located in the small intestine, facilitates glucose absorption, its inhibition significantly impacts postprandial glucose levels more than α-amylase inhibition, which occurs in saliva and the pancreas[43,44]. FrE exhibited potent α-glucosidase inhibition (IC_{50} 0.3 µg/mL), surpassing α-amylase inhibition, aligning with its role in mitigating postprandial hyperglycemia. The superior activity of FrE highlights its potential to reduce post-meal glucose spikes with fewer off-target effects, a critical advantage over broad-spectrum glucose inhibitors like acarbose.

MT modulate glucose uptake and consumption to modulate insulin sensitivity

Glucose uptake and consumption assays emphasize the ability of a fraction-enriched extract (i.e., FrE) to enhance glucose disposal, thereby reducing the risk of insulin resistance. FrE significantly enhanced glucose uptake in

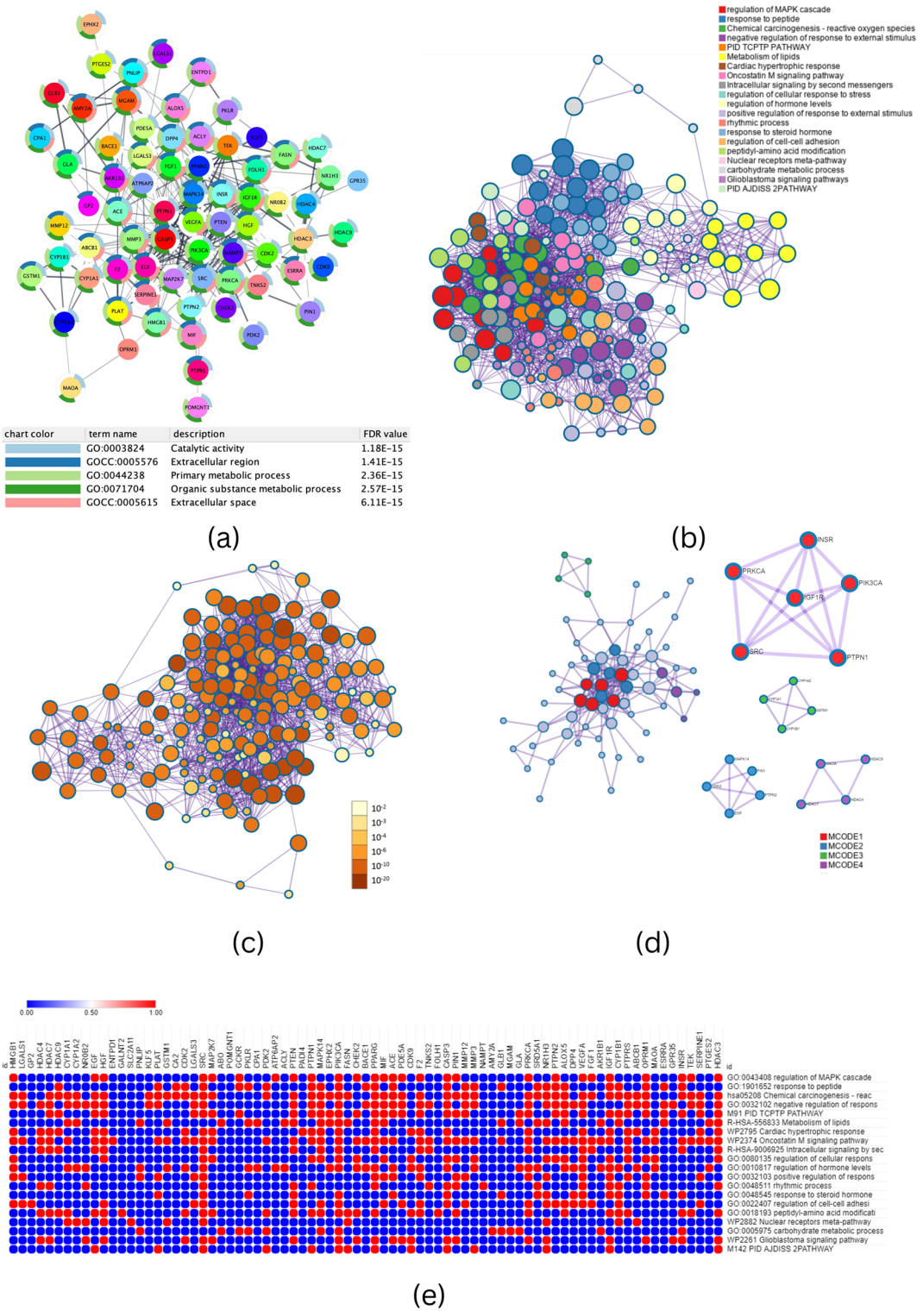

Fig. 4. Functional Association Enrichment Analysis of MT targets. **(a)** Protein-Protein interaction Network of targets related to diabetes interacting with MT molecules the borders in pie format show functional annotation. **(b)** Network of enriched terms colored by cluster ID, where nodes that share the same cluster ID are typically close to each other (BP), molecular functions (MF), and cellular processes (CC). **(c)** Network of enriched terms colored by *p*-value, where terms containing more genes tend to have a more significant *p*-value. **(d)** Protein-protein interaction enrichment analysis of MT and MCODE components identified in the gene lists. **(e)** Gene-functional annotation heatmap.

GO	Description	Count	%	Log10 (*P*)	Log10 (q)
GO:0043408	Regulation of MAPK cascade	21	26.58	−16.22	−11.87
GO:1,901,652	Response to peptide	18	22.78	−15.81	−11.76
hsa05208	Chemical carcinogenesis - reactive oxygen species	14	17.72	−15.12	−11.25
GO:0032102	Negative regulation of response to external stimulus	17	21.52	−14.43	−10.92
M91	PID TCPTP pathway	8	10.13	−12.78	−9.55
R-HSA-556,833	Metabolism of lipids	18	22.78	−12.23	−9.18
WP2795	Cardiac hypertrophic response	8	10.13	−11.78	−8.75
WP2374	Oncostatin M signalling pathway	8	10.13	−11.17	−8.24
R-HSA-9,006,925	Intracellular signalling by second messengers	12	15.19	−10.54	−7.72
GO:0080135	Regulation of cellular response to stress	16	20.25	−10.50	−7.69
GO:0010817	Regulation of hormone levels	14	17.72	−9.99	−7.31
GO:0032103	Positive regulation of Response to external stimulus	14	17.72	−9.94	−7.28
GO:0048511	Rhythmic process	11	13.92	−9.76	−7.12
GO:0048545	Response to steroid hormone	11	13.92	−9.61	−7.00
GO:0022407	Regulation of cell-cell adhesion	13	16.46	−9.32	−6.76
GO:0018193	Peptidyl-amino acid modification	15	18.99	−9.24	−6.71
WP2882	Nuclear receptors meta-pathway	11	13.92	−9.21	−6.69
GO:0005975	Carbohydrate metabolic process	12	15.19	−8.77	−6.33
WP2261	Glioblastoma signalling pathways	7	8.86	−8.65	−6.24

Table 8. Top 20 clusters with their representative enriched terms associated with the MT target proteins involved in diabetes.

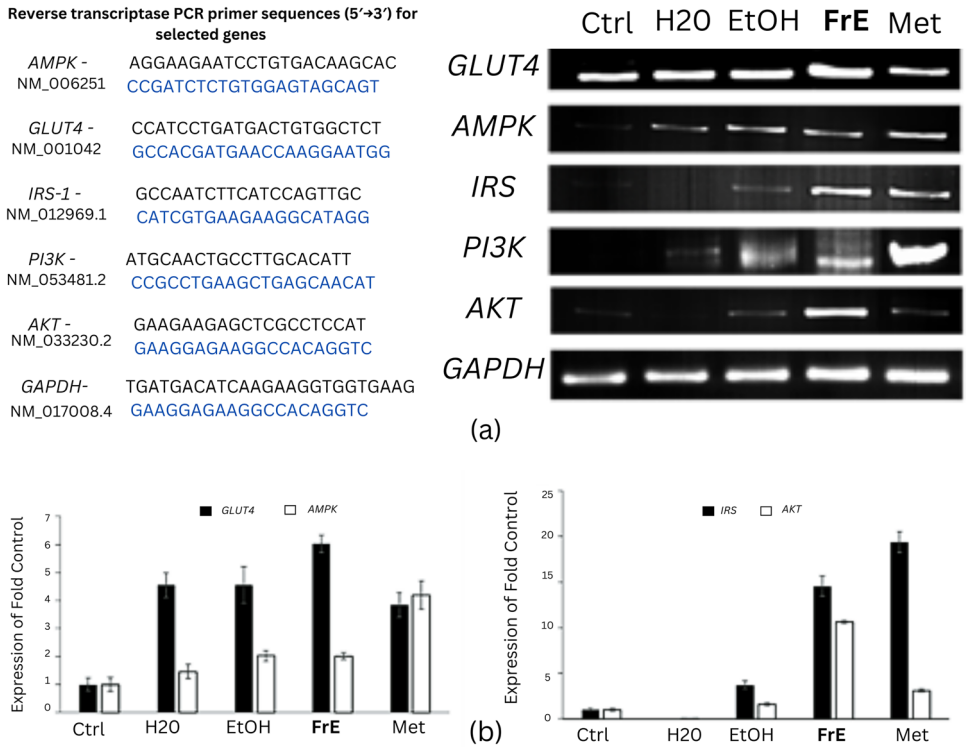

Fig. 5. MT induces insulin mediated glucose transport related gene expression in L6 myotubes. **(a)** Gel doc representation of expression of glucose metabolism genes on L6 myotubes after treating with MT extracts, fractions, and metformin at 100 µg/mL showing GLUT4, AMPK, IRS, PI3K and AKT gene expression using GAPDH as the internal control. **(b)** The relative expression of insulin signalling related genes accessed by image intensity analysis expressed as fold change compared to control. FrE represents the EtOH extract partitioned with EtOAc.

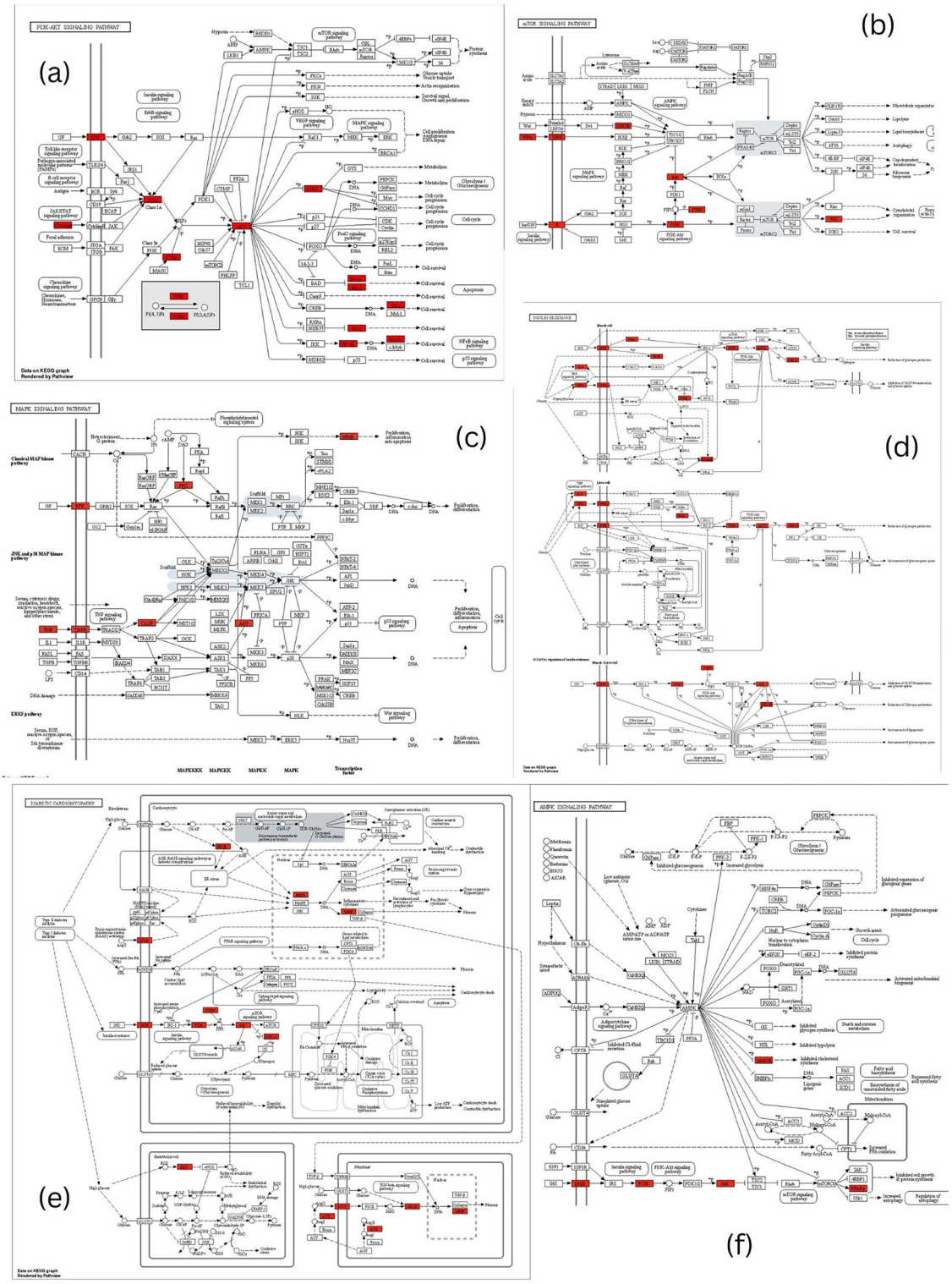

Fig. 6. Pathway Analysis of MT targets associated with T2DM. **(a)** PI3K-AKT signalling pathway. **(b)** mTOR signalling pathway. **(c)** MAP-kinase signalling pathway. **(d)** Insulin resistance pathway. **(e)** Diabetic cardiomyopathy **(f)** AMPK pathway. The red nodes in the pathway represent targets which interact with MT molecules.The KEGG pathway maps were obtained from KEGG database (https://www.kegg.jp/kegg/pathway.html) rendered using Pathview.

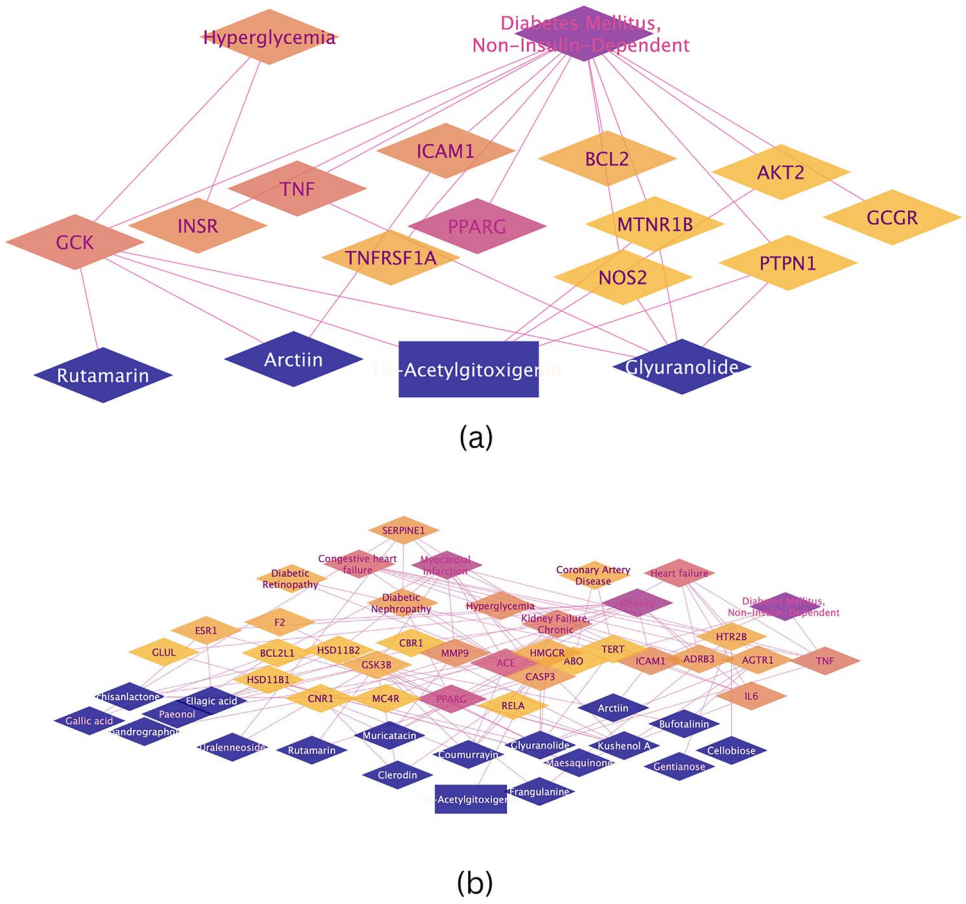

Fig. 7. Combination Synergy Network Analysis based on neighbourhood approach. **(a)** Multi-molecular combination network of compound-target-disease against diabetes. **(b)** Multi-molecular combination network of compound-target-disease against diabetes with cardiac protection mechanism.

L6 myotubes (3.67 ± 0.23-fold vs. control) and suppressed adipocyte glucose consumption (IC_{50} 6.78 μg/mL), suggesting the dual benefits of promoting peripheral glucose utilization while limiting lipid accumulation in adipose tissue, a key driver of insulin resistance46. Notably, FrE exceeded metformin in glucose uptake efficacy, implying insulin-mimetic or sensitizing effects. This aligns with its upregulation of the GLUT4, AMPK, and PI3K/AKT pathways in L6 cells, which are central to skeletal muscle glucose homeostasis mechanism48.

MT in pancreatic β-Cell protection and insulin secretion

INS-1 β-cell protection assays assessed MT's therapeutic potential in diabetes management. Oxidative stress-induced β-cell apoptosis is a key factor in Type 2 Diabetes Mellitus (T2DM) progression. The ability of FrE to protect β-cells against H_2O_2-induced apoptosis through caspase-3 inhibition highlights its role in β-cell preservation. Additionally, the enhancement of insulin secretion by FrE suggests a direct stimulatory effect on β-cell function, further supporting its antidiabetic potential. FrE protected INS-1 β-cells from H_2O_2-induced apoptosis (30.65 ± 3.54% caspase-3 inhibition) and stimulated insulin secretion (2512.11 ± 26 μIU/mL), comparable to metformin. These effects are mediated through the PI3K/AKT and NRF2-ARE pathways, which mitigate oxidative stress and restore β-cell function[49–52]. The dual capacity to enhance insulin secretion while preserving β-cell viability also addresses a critical gap in current therapeutic options, which often fail to halt β-cell degeneration in T2DM.

MT targets Multi-Target networks against diabetes

Unlike single-target drugs, such as metformin (primarily activating AMPK) and acarbose (inhibiting α-glucosidase), MT as a complex of 26 medicinal plants and innumerable metabolites, exhibits multi-target mechanisms of action. It enhances glucose uptake, stimulates insulin secretion, protects β-cells, and inhibits digestive enzymes, offering a comprehensive strategy for blood sugar regulation. These findings position MT as a promising multifunctional antidiabetic agent, necessitating further in vivo and clinical studies to establish translational potential. Network analysis identified the interactions of FrE with 745 nodes, including hub targets like MAPK14, CA2, PPARG, and GSK3B. Carbonic anhydrase isoforms (CA1, CA2, and CA4) and TNKS1 emerged as novel targets, linking MT to hepatic gluconeogenesis suppression and GLUT4-mediated insulin sensitivity[47]. Key metabolites, including gallic acid, ellagic acid, and 16-acetylgitoxigenin, modulated the

PI3K/AKT/GLUT4 and AMPK/mTOR pathways, synergistically enhancing glucose uptake[53] and suppressing gluconeogenesis[54],. Crosstalk between these pathways restores energy homeostasis, a hallmark of effective antidiabetic agents[49–52]. SwissADME analysis signifies drug-likeness for most FrE metabolites (bioavailability score: 0.6; Lipinski violations: 0.16). However, compounds like gentianose and arctiin showed reduced bioavailability, guiding future optimization efforts. The structural diversity of the MT metabolites enables multi-target engagement, circumventing the biological limitations of single-agent therapies.

Findings from this study align with prior research on the 26 medicinal plants comprising the Wang-Nam-Yen preparation, which demonstrated antidiabetic activity through the terpenoid and flavonoid constituents[55]. Network analysis identified MT bioactive metabolites targeting multiple diabetes-related pathways, including diabetic retinopathy, nephropathy, and cardiovascular diseases[24]. The multi-molecular combination network (MCN) of MT (Fig. 7a) reveals interactions with 14 diabetes-related sites through 22 metabolites. Compounds such as rutamarin, arctiin, 16-acetylgitoxigenin, and glyuranolide interact with key glucose metabolism regulators, including GCK, INS, TNF, and PPARG[56]. Rutamarin's interaction with protein tyrosine phosphatase 1B (PTP1B) enhances insulin-induced GLUT4 translocation through the PI3K/AKT pathway, increasing glucose uptake. Additionally, network mapping identified cardio-protective interactions involving phenolics such as gallic acid, ellagic acid, and neo-andrographolide, which target ACE, TNF, MMP9, and GSK3B - key mediators of diabetic cardiomyopathy. Clinical studies associate T2DM with elevated MMP-7 and MMP-12 levels, contributing to atherosclerosis and coronary events[49–52]. Network analysis suggests that MT may mitigate diabetes-associated cardiomyopathy by modulating MMP9, PIK3CA, AGTR1, ACE, INSR, AKT2, PTEN, PRKCB, RELA, and GSK3B. The enrichment of the MAPK, FoxO, HIF-1, and PI3K-Akt signalling pathways (Table 7) suggests that MT (FrE) targets critical hubs governing cellular proliferation, stress adaptation, and metabolic regulation. The prominence of MAPK signalling in KEGG[32] pathways (Table 7) and GO clusters (Table 8) aligns with its established role in insulin resistance and inflammation, key drivers of diabetes pathogenesis. Similarly, the PI3K-Akt and FoxO pathways, central to glucose homeostasis and apoptosis, further implicate MT in modulating insulin signalling and β-cell survival.

The significant enrichment of pathways like "endocrine resistance" and "AGE-RAGE signalling in diabetic complications" (Table 7) highlights the potential intersections between diabetes progression and therapeutic resistance or oxidative stress. This is reinforced by the cluster "chemical carcinogenesis - reactive oxygen species" (Table 8), linking oxidative damage to diabetic complications. The association of lipid metabolism and carbohydrate processes (Table 8) underscores the potential role of MT in addressing metabolic dysregulation, another hallmark of diabetes.

Clusters such as "regulation of hormone levels" and "response to peptide" (Table 8) may reflect MT's influence on insulin and incretin signalling, while terms like "negative regulation of response to external stimulus" suggest protective mechanisms against stressors exacerbating diabetes. The overlap between the enriched pathways (e.g., MAPK and AMPK) and disease-specific processes (e.g., cardiac hypertrophy) implies systemic effects, possibly connecting diabetes to cardiovascular comorbidities. The statistical robustness of these findings (e.g., FDR < 1E-14 for top pathways) strengthens confidence in the multi-target engagement capacity of MT. However, further experimentation is needed to establish causality. Collectively, these results position the multimetabolite composition of MT as a modulator of interconnected signalling networks influencing diabetes progression, and offering insights for therapeutic strategies targeting metabolic, inflammatory, and stress-response pathways.

Mechanistic insights: PI3K/AKT/GLUT4 signalling and insulin sensitivity

The PI3K/AKT/GLUT4 pathway plays a crucial role in glucose metabolism, enhancing glucose consumption and alleviating insulin resistance in obesity-related diabetes[8]. Skeletal muscle glucose uptake, primarily mediated by GLUT4, is essential for systemic glucose homeostasis. Upregulation of GLUT4, AMPK, AKT, and INS mRNA expression supports increased glucose uptake through the insulin and AMPK pathways. Activation of the IRS1-PI3K-AKT-GLUT4 pathway in L6 cells further supports reduced insulin resistance and enhanced glucose absorption. Up-regulation was observed for IRS, PI3K, and Akt gene expression in cells treated with MT extracts (Figs. 6a,-**b**). Based on this evidence, the cells showed enhanced glucose uptake through the insulin and AMPK pathways. MT extracts might therefore enhance glucose uptake, which is then translocated into the cells through the GLUT4 receptor, and subsequently metabolized through AMPK activation[56]. AMPK stimulation promotes the AMP/ATP ratio and increases intracellular calcium levels[57]. The AMPK domain regulates glucose uptake by TBC1D4 and TBC1D1 phosphorylation, this allows Rab proteins and glucose transport 4 (GLUT4) translocation, improving glucose uptake into the cells[58]. Interestingly, insulin plays a critical role in glucose regulation[59]. In addition, insulin secretion is activated by the insulin receptor (IRS) PI3K and AKT[54]. This correlates with the high level of expression of these genes in MT-treated L6 cells in this study. The glucose uptake by skeletal muscle cells, and the upregulation of GLUT4, AMPK, AKT, and IRS gene expression after MT treatment, similar to that of metformin, suggests a beneficial role of the MT metabolites in overcoming insulin resistance and diabetic complications by modulating the PI3K-AKT/AMPK/GLUT4 signalling cascade[48].The experimental observations align with network pharmacology predictions, which indicate enrichment in insulin secretion (GO:0030073) and PI3K/AKT pathway involvement. Prior studies on β-cells subjected to STZ-induced damage suggest that the PI3K/AKT/insulin pathway plays a protective role against apoptosis[60]. Moreover, the NRF2 pathway, known for regulating oxidative stress, modulates apoptosis through enzyme activity, receptor signalling, and ROS reduction[61]. Enrichment of the NRF2-ARE regulatory network (WP4357) and insulin signalling (WP481) highlights the antioxidative and insulin-preserving mechanisms of MT extracts supported by previous reports which support Nrf2 activation through the actions of metabolites such as naringin and epigallocatechin-3-gallate[62].

AMPK/PI3K-AKT crosstalk and energy homeostasis restoration

The results also reveal that the structural diversity of the metabolites in MT are operating at multiple sites and mechanisms of action to combat T2DM. Metformin increases glucose uptake in L6 myotube skeletal muscle cells[8]. This suggests that a combination of MT bioactive metabolites, i.e., gallic acid, kushenol A, 7-*O*-methylaromadendrin, paeonol, and astilbin may be more effective than a single compound, metformin, through a multi-combinatorial homeostatic mechanism of action[49–52]. The MT metabolites interact with TNFRSF1A, TNF, INSR, AKT2, CASP3, PRKCB, and RELA, which are all linked to MAP kinase signalling. Compound analysis further reveals that MT metabolites, particularly glyuranolide, interact with TNF, influencing insulin resistance. The target compound network highlights the AMPK pathway interactions (Fig. 5f), including PPARG engagement by bioactives such as schisanlactone E, kushenol A, muricatacin, 16-acetylgitoxigenin, and gallic acid. AMPK signalling enhances insulin sensitivity, increases GLUT4 expression, and stimulates glucose uptake in muscle cells while concurrently inhibiting mTOR to promote autophagy and mitigate insulin resistance. The crosstalk between the AMPK, PI3K-AKT, and insulin pathways suggests a metabolic shift that restores energy homeostasis. PPI and pathway enrichment analyses revealed the role of MT in mitigating diabetic cardiomyopathy through the modulation of MMP9, TNF, and AGTR1. The AGE-RAGE and HIF-1 signalling pathways, enriched in cells treated with FrE, further underscore its potential to address vascular and metabolic comorbidities.

The superior efficacy of FrE over metformin in glucose uptake assays, coupled with its β-cell protective effects, positions MT as a holistic alternative or adjunct to current therapies. The enrichment of the MAPK, FoxO, and PI3K-AKT pathways in proteomic networks ($p < 0.05$; FDR < 0.05) mirrors clinical T2DM signatures, suggesting translatability. However, in vivo assessment is critical to examine these effects in physiological contexts of metabolic dysregulation. In vivo studies will be a key focus of future studies and will also prioritize phosphoproteomics and single-cell transcriptomics to resolve cell-type-specific signalling dynamics through longer-term in vivo studies assessing the impact of FrEon diabetic cardiomyopathy and nephropathy.

Conclusions

This study provides a comprehensive molecular characterization of the antidiabetic potential of Mathurameha (MT) extracts and fractions. The ethyl acetate fraction (FrE) demonstrated the most potent activity, exhibiting significant α-glucosidase inhibition (IC_{50} 0.3 µg/mL) and enhancing glucose uptake in L6 myotubes (3.67 ± 0.23-fold) and 3T3-L1 adipocytes (IC_{50} 6.78 µg/mL). Additionally, FrE stimulated insulin secretion (1.42-fold), comparable to metformin (1.46-fold) at 100 µg/mL in INS-1 pancreatic β-cells. Notably, FrE protected INS-1 cells against H_2O_2-induced apoptosis (30.65 ± 3.54%) through partial caspase-3 inhibition, demonstrating superior cytoprotective effects compared to metformin (65.06 ± 2.32%).

Metabolomic profiling (LC-MS-QTOF) identified 73 known bioactive metabolites across the aqueous and ethanol extracts and the FrE fraction, with compounds such as ellagic acid, kushenol A, gallic acid, arctin, neoandrographolide, astilbin, paenol, muricatacin, coumarrayin, and zingerone playing key pharmacological roles. Network pharmacology and pathway enrichment analyses identified critical molecular targets (GSK3β, GLUT4, PPARG, INSR, AKT2, CASP3, and MMP9) and highlighted the involvement of key pathways, including MAPK, FoxO, HIF-1, and PI3K-Akt, suggesting that MT modulates the PI3K-AKT/AMPK/GLUT4 signalling axis. Gene expression studies in L6 myotubes treated with FrE further demonstrated significant upregulation of GLUT4, AMPK, IRS, PI3K, and AKT genes, reinforcing its role in glucose metabolism regulation.

Future research should focus on developing standardized formulations enriched with the most bioactive metabolites to optimize therapeutic efficacy. INS-1, L6, and 3T3-L1 are standard in vitro models; however, future work will involve human-derived organoids and preclinical mouse models to increase translational relevance In vivo assessment through pharmacokinetic studies, RT-PCR, Western blotting, and omics-based approaches (phosphoproteomics and transcriptomics) will further elucidate molecular mechanisms of MT. Sustainable sourcing of the 26 MT components is a practical challenge. Cultivation and quality assurance strategies are currently being explored to address this vital issue. These concerns are designed to ensure the long-term quality, safety, efficacy, consistency, and availability of MT-based interventions for type 2 Diabetes Mellitus.

Data availability

The datasets generated during and/or analyzed during the current study are available from the corresponding author upon reasonable request.

Received: 26 March 2025; Accepted: 8 August 2025
Published online: 17 August 2025

References

1. Dahlén, A. D. et al. Trends in antidiabetic drug discovery: FDA approved drugs, new drugs in clinical trials and global sales. *Front. Pharmacol.* **12** https://doi.org/10.3389/fphar.2021.807548 (2022). https://www.frontiersin.org/articles/ (accessed 26 Nov2022).
2. González, P., Lozano, P., Ros, G. & Solano, F. Hyperglycemia and oxidative stress: an integral, updated and critical overview of their metabolic interconnections. *Int. J. Mol. Sci.* **24**, 9352 (2023).
3. Clapham, J. C. Sixty years of drug discovery for type 2 diabetes: where are we now?? In *Type 2 Diabetes: Methods and Protocols* (ed. Stocker, C. J.) 1–30 (Springer, 2020).
4. Gerber, P. A. & Rutter, G. A. The role of oxidative stress and hypoxia in pancreatic Beta-Cell dysfunction in diabetes mellitus. *Antioxid. Redox Signal.* **26**, 501–518 (2017).
5. Mirabelli, M., Chiefari, E., Puccio, L., Foti, D. P. & Brunetti, A. Potential benefits and harms of novel antidiabetic drugs during COVID-19 crisis. *Int. J. Environ. Res. Public. Health.* **17**, 3664 (2020).
6. Choudhury, H. et al. An update on natural compounds in the remedy of diabetes mellitus: A systematic review. *J. Tradit Complement. Med.* **8**, 361–376 (2018).

7. Eawsakul, K. et al. Computational study and in vitro alpha-glucosidase inhibitory effects of medicinal plants from a Thai folk remedy. *Heliyon* **7**, e08078 (2021).
8. Balachandran, A. et al. Marsupsin isolated from polyherbal product ABPA rejuvenates insulin resistance in L6 skeletal muscle cell line via IRS1-PI3K-AKT-GLUT4 signaling pathway. *FASEB J.* 36. https://doi.org/10.1096/fasebj.2022.36.S1.00R79 (2022).
9. Chayarop, K. et al. Hypoglycaemic activity of mathurameha, a Thai traditional herbal formula aqueous extract, and its effect on biochemical profiles of streptozotocin-nicotinamide-induced diabetic rats. *BMC Complement. Altern. Med.* **17**, 343 (2017).
10. Permphol, P. et al. Efficacy and safety of Mathurameha for type 2 diabetes mellitus treatment. *TMJ* **16**, 589–599 (2016).
11. Chayarop, K. et al. Anti-diabetic activity and acute toxicity of Thai traditional herbal formula, Mathura Meha aqueous extract. *Planta Med.* **80**, P2B102 (2014).
12. Pandeya, P. R. et al. Antiobesity Activity of Two Polyherbal Formulations in High-Fat Diet-Induced Obese C57BL/6J Mice. *BioMed Res Int* ; 2022: e9120259. (2022).
13. Pandeya, P. R. et al. 18KHT01, a potent Anti-Obesity polyherbal formulation. *Front. Pharmacol.* 12. https://doi.org/10.3389/fphar.2021.807081 (2021).
14. Huang, X-J. et al. Systems pharmacology-based dissection of mechanisms of Tibetan medicinal compound Ruteng as an effective treatment for collagen-induced arthritis rats. *J. Ethnopharmacol.* **272**, 113953 (2021).
15. Peng, M. et al. Integrative Pharmacology reveals the mechanisms of Erzhi pill, a traditional Chinese formulation, against diabetic cardiomyopathy. *J. Ethnopharmacol.* **296**, 115474 (2022).
16. Aluksanasuwan, S. et al. SWATH-proteomics reveals mathurameha, a traditional anti-diabetic herbal formula, attenuates high glucose-induced endothelial dysfunction through the EGF/NO/IL-1β regulatory axis. *J. Proteom.* **306**, 105263 (2024).
17. Somsuan, K. et al. Mathurameha ameliorates cardiovascular complications in high-fat diet/low-dose streptozotocin-induced type 2 diabetic rats: insights from histological and proteomic analysis. *J. Mol. Histol.* https://doi.org/10.1007/s10735-024-10258-6 (2024).
18. Piriyapornpipat, S. & Wasanat, P. A comparison between Mathurameha and Metformin in the result of efficacy and safety among new-onset type 2 diabetes. *J. Thai Tradit Altern. Med.* **18**, 478–495 (2020).
19. Taneera, J. et al. Reduced expression of Chl1 gene impairs insulin secretion by Down-Regulating the expression of key molecules of β-cell function. *Exp. Clin. Endocrinol. Diabetes Off J. Ger. Soc. Endocrinol. Ger. Diabetes Assoc.* **129**, 864–872 (2021).
20. El-Huneidi, W. et al. Carnosic acid protects INS-1 β-Cells against Streptozotocin-Induced damage by inhibiting apoptosis and improving insulin secretion and glucose uptake. *Molecules* **27**, 2102 (2022).
21. Veluthakal, R., Arora, D. K., Goalstone, M. L., Kowluru, R. A. & Kowluru, A. Metabolic stress induces Caspase-3 mediated degradation and inactivation of Farnesyl and geranylgeranyl transferase activities in pancreatic β-Cells. *Cell. Physiol. Biochem.* **39**, 2110–2120 (2016).
22. Odeyemi, S. & Dewar, J. In vitro antidiabetic activity affecting glucose uptake in HepG2 cells following their exposure to extracts of lauridia Tetragona (L.f.) R.H. Archer. *Processes* **8**, 33 (2020).
23. Banerjee, S. et al. Combining LC-MS/MS profiles with network Pharmacology to predict molecular mechanisms of the hyperlipidemic activity of lagenaria siceraria stand. *J. Ethnopharmacol.* **300**, 115633 (2022).
24. Gilson, M. K. et al. BindingDB in 2015: A public database for medicinal chemistry, computational chemistry and systems Pharmacology. *Nucleic Acids Res.* **44**, D1045–D1053 (2016).
25. Daina, A., Michielin, O. & Zoete, V. SwissTargetPrediction: updated data and new features for efficient prediction of protein targets of small molecules. *Nucleic Acids Res.* **47**, W357–W364 (2019).
26. Shaikh, F., Tai, H. K., Desai, N. & Siu, S. W. I. LigTMap: ligand and structure-based target identification and activity prediction for small molecular compounds. *J. Cheminformatics*. **13**, 44 (2021).
27. Daina, A., Michielin, O. & Zoete, V. SwissADME: a free web tool to evaluate pharmacokinetics, drug-likeness and medicinal chemistry friendliness of small molecules. *Sci. Rep.* **7**, 42717 (2017).
28. Piñero, J., Saüch, J., Sanz, F. & Furlong, L. I. The disgenet cytoscape app: exploring and visualizing disease genomics data. *Comput. Struct. Biotechnol. J.* **19**, 2960–2967 (2021).
29. Szklarczyk, D. et al. The STRING database in 2017: quality-controlled protein–protein association networks, made broadly accessible. *Nucleic Acids Res.* **45**, D362–D368 (2017).
30. Xia, J., Gill, E. E. & Hancock, R. E. W. NetworkAnalyst for statistical, visual and network-based meta-analysis of gene expression data. *Nat. Protoc.* **10**, 823–844 (2015).
31. Sherman, B. T. et al. DAVID: a web server for functional enrichment analysis and functional annotation of gene lists (2021 update). *Nucleic Acids Res.* **50**, W216–W221 (2022).
32. Kanehisa, M., Furumichi, M., Sato, Y., Matsuura, Y. & Ishiguro-Watanabe, M. KEGG: biological systems database as a model of the real world. *Nucleic Acids Res.* **53**, D672–D677 (2025).
33. Kanehisa, M. Toward Understanding the origin and evolution of cellular organisms. *Protein Sci. Publ Protein Soc.* **28**, 1947–1951 (2019).
34. Luo, W. & Brouwer, C. Pathview: an r/bioconductor package for pathway-based data integration and visualization. *Bioinforma Oxf. Engl.* **29**, 1830–1831 (2013).
35. Bader, G. D. & Hogue, C. W. V. An automated method for finding molecular complexes in large protein interaction networks. *BMC Bioinform.* **4**, 2 (2003).
36. Zhou, Y. et al. Metascape provides a biologist-oriented resource for the analysis of systems-level datasets. *Nat. Commun.* **10**, 1523 (2019).
37. Li, T. et al. A scored human protein-protein interaction network to catalyze genomic interpretation. *Nat. Methods.* **14**, 61–64 (2017).
38. Stark, C. et al. BioGRID: a general repository for interaction datasets. *Nucleic Acids Res.* **34**, D535–539 (2006).
39. Banerjee, S., Bhattacharjee, P., Kar, A. & Mukherjee, P. K. LC-MS/MS analysis and network Pharmacology of trigonella foenum-graecum- a plant from ayurveda against hyperlipidemia and hyperglycemia with combination synergy. *Phytomedicine* **60**, 152944. https://doi.org/10.1016/j.phymed.2019.152944 (2019).
40. Shannon, P. et al. Cytoscape: a software environment for integrated models of biomolecular interaction networks. *Genome Res.* **13**, 2498–2504 (2003).
41. Dandekar, P. D. et al. Insights into the Inhibition mechanism of human pancreatic α-Amylase, a type 2 diabetes target, by dehydrodieugenol B isolated from ocimum tenuiflorum. *ACS Omega*. **6**, 1780–1786 (2021).
42. Ismail, I. S. The role of carbonic anhydrase in hepatic glucose production. *Curr. Diabetes Rev.* **14**, 108–112 (2018).
43. Ismail, I. S. Metformin-carbonic anhydrase interaction facilitate lactate accumulation in type 2 diabetes. *Diabetes Manag.* **7**, 337–342 (2017).
44. Wang, N. et al. Metabolite profiling of traditional Chinese medicine XIAOPI formula: an integrated strategy based on UPLC-Q-Orbitrap MS combined with network Pharmacology analysis. *Biomed. Pharmacother.* **121**, 109569 (2020).
45. Wang, P. et al. Applying cooperative module pair analysis to uncover compatibility mechanism of fangjis: an example of Wenxin Keli Decoction. *J. Ethnopharmacol.* **278**, 114214 (2021).
46. Jubaidi, F. F. et al. The role of PKC-MAPK signalling pathways in the development of Hyperglycemia-Induced cardiovascular complications. *Int. J. Mol. Sci.* **23**, 8582 (2022).

47. He, L. et al. Chemical profile and potential mechanisms of Huo-Tan-Chu-Shi Decoction in the treatment of coronary heart disease by UHPLC-Q/TOF-MS in combination with network Pharmacology analysis and experimental verification. *J. Chromatogr. B.* **1175**, 122729 (2021).
48. Meng, Q. et al. IRS1/PI3K/AKT pathway signal involved in the regulation of glycolipid metabolic abnormalities by mulberry (Morus Alba L.) leaf extracts in 3T3-L1 adipocytes. *Chin. Med.* **15**, 1 (2020).
49. Gandhi, G. R. et al. Gallic acid attenuates high-fat diet fed-streptozotocin-induced insulin resistance via partial agonism of PPARγ in experimental type 2 diabetic rats and enhances glucose uptake through translocation and activation of GLUT4 in PI3K/p-Akt signaling pathway. *Eur. J. Pharmacol.* **745**, 201–216 (2014).
50. Liao, J. et al. Andrographolide promotes uptake of glucose and GLUT4 transport through the PKC pathway in L6 cells. *Pharmaceuticals* **15**, 1346 (2022).
51. Variya, B. C., Bakrania, A. K. & Patel, S. S. Antidiabetic potential of Gallic acid from emblica officinalis: improved glucose transporters and insulin sensitivity through PPAR-γ and Akt signaling. *Phytomedicine Int. J. Phytother Phytopharm*. **73**, 152906 (2020).
52. Zhou, M., Li, G., Zhu, L., Zhou, H. & Lu, L. Arctiin attenuates high glucose-induced human retinal capillary endothelial cell proliferation by regulating ROCK1/PTEN/PI3K/Akt/VEGF pathway in vitro. *J. Cell. Mol. Med.* **24**, 5695–5706 (2020).
53. Chen, Z. et al. Anthocyanins from dietary black soybean potentiate glucose uptake in L6 rat skeletal muscle cells via up-regulating phosphorylated Akt and GLUT4. *J. Funct. Foods*. **52**, 663–669 (2019).
54. De Meyts, P. et al. The Insulin Receptor and Its Signal Transduction Network. In: Feingold KR, Anawalt B, Blackman MR, Boyce A, Chrousos G, Corpas E (eds). *Endotext*. MDText.com, Inc.: South Dartmouth (MA), (2000). http://www.ncbi.nlm.nih.gov/books/NBK378978/ (accessed 29 Aug2023).
55. Rachpirom, M. et al. Antidiabetic activities of medicinal plants in traditional recipes and candidate antidiabetic compounds from hydnophytum formicarum jack. Tubers. *Pharmacogn Res.* **14**, 89–99 (2022).
56. Entezari, M. et al. AMPK signaling in diabetes mellitus, insulin resistance and diabetic complications: A pre-clinical and clinical investigation. *Biomed. Pharmacother*. **146**, 112563 (2022).
57. O' Neill, C. PI3-kinase/Akt/mTOR signaling: impaired on/off switches in aging, cognitive decline and alzheimer's disease. *Exp. Gerontol.* **48**, 647–653 (2013).
58. Dhanya, R., Arya, A. D., Nisha, P. & Jayamurthy, P. Quercetin, a lead compound against type 2 diabetes ameliorates glucose uptake via AMPK pathway in skeletal muscle cell line. *Front. Pharmacol.* **8**, 336 (2017).
59. Zhang, Y. et al. +)-Rutamarin as a dual inducer of both GLUT4 translocation and expression efficiently ameliorates glucose homeostasis in Insulin-Resistant mice. *PLoS ONE*. **7**, e31811 (2012).
60. Savova, M. S., Mihaylova, L. V., Tews, D., Wabitsch, M. & Georgiev, M. I. Targeting PI3K/AKT signaling pathway in obesity. *Biomed. Pharmacother*. **159**, 114244 (2023).
61. Sireesh, D., Dhamodharan, U., Ezhilarasi, K., Vijay, V. & Ramkumar, K. M. Association of NF-E2 related factor 2 (Nrf2) and inflammatory cytokines in recent onset type 2 diabetes mellitus. *Sci. Rep.* **8**, 5126 (2018).
62. Suraweera, L., Rupasinghe, T., Dellaire, H. P. V. & Xu, G. Regulation of Nrf2/ARE pathway by dietary flavonoids: A friend or foe for cancer management?? *Antioxidants* **9**, 973 (2020).

Acknowledgements

The authors thank the Medicinal Plants Innovation Center of Mae Fah Luang University and Mae Fah Luang University for the provision of laboratory facilities.

Author contributions

Subhadip Banerjee- contributed in conceptualization, methodology, assessment strategies, network pharmacology analysis, LC-MS study, data interpretation, writing the original draft, reviewing and editing, and visualization; Wuttichai Jaidee- did the extraction, fractionation, LC-MS analysis, data curation, writing, reviewing, editing, and visualization; Narawadee Rujanapun- analyzed the cell line studies, conducted data curation, writing, and visualization; Thidarat Duangyod, Pravaree Phuneerub- prepared the formulation, acquired the medicinal plants; Tharakorn Maneerat- analyzed the chemometric and chemical analysis; Kulwadee Malee, Siam Popluechai- did biological data interpretation and biochemical methods validation; Virayu Suthiphasilp- contributed in chemical analysis; Panupong Puttarak, Poonsit Hiransai - helped in reviewing and editing; Surat Laphookhieo- contributed in project administration and funding acquisition; Salfarina Ramli-reviewing and editing; Wim Vanden Berghe-helped in data analysis, bioinformatic data analysis; Geoffrey A. Cordell- reviewed and edited the manuscript; Rawiwan Charoensup- contributed by initiating the project, providing the funding, administering the project, writing the original draft, reviewing and editing, conceptualization, and developing the overall methodology.

Funding

This research was funded by the Thailand Science Research and Innovation Fund (Grant number: DBG6280007), the Permanent Secretary of the Ministry of Higher Education, Science, Research, and Innovation (Grant number: F01-683R-17-046), and the Hub of Knowledge: Herbs for Sustainable Health and Well-being Consortium and supported by the National Research Council of Thailand (Grant number: N35E680089). Subhadip Banerjee acknowledges the postdoctoral fellowship provided by Mae Fah Luang University (Grant number: 04/2025).

Declarations

Competing interests

The authors declare no competing interests.

Additional information

Supplementary Information The online version contains supplementary material available at https://doi.org/10.1038/s41598-025-15556-x.

Correspondence and requests for materials should be addressed to R.C.